Chaos, Solitons and Fractals 147 (2021) 110998

Contents lists available at ScienceDirect

Chaos, Solitons and Fractals

Nonlinear Science, and Nonequilibrium and Complex Phenomena

journal homepage: www.elsevier.com/locate/chaos

Chaos and hyperchaos arising from the destruction of multifrequency tori

N.V. Stankevich[a,b,c,d,*], A.P. Kuznetsov[a], E.P. Seleznev[a,e]

[a] Kotel'nikov's Institute of Radio-Engineering and Electronics of RAS, Saratov Branch, Zelenaya 38, Saratov, 410019, Russian Federation
[b] HSE University, Bolshaya Pecherskaya str. 25/12, Nizhny Novgorod, 603155, Russian Federation
[c] St. Petersburg State University, Universitetskiy proezd,28, Pterhof, Saint-Petersburg, 198504, Russian Federation
[d] Yuri Gagarin State Technical University of Saratov, Politehnicheskaya 77, Saratov, 410054, Russian Federation
[e] Chernyshevsky Saratov State University, Astrakhanskaya, 83, Saratov, 410012, Russian Federation

ARTICLE INFO

Article history:
Received 1 April 2021
Accepted 19 April 2021

Keywords:
Multi-contour generator
Chaos
Hyperchaos
Quasiperiodic oscillations
Lyapunov exponents

ABSTRACT

Appearance of chaotic dynamics as a result of multi-frequency tori destruction is carried out on the example of a model of a multimode generator. Quasiperiodic bifurcations occurring with multi-frequency tori are discussed in the context of the Landau-Hopf scenario. Structure of the parameter space is studied, areas with various chaotic dynamics, including chaos and hyperchaos, are revealed. Scenarios of the development of chaotic dynamics are described, the features of chaotic signals of various types are revealed.

1. Introduction

Quasiperiodic oscillations are typical attribute of the dynamics of non-autonomous systems and ensembles of coupled self-sustaining oscillators [1–5]. Quasiperiodic oscillations can be classified according to the number of independent frequencies involved in the dynamics. In the simplest case, a system is characterized by two incommensurate frequencies; then attractor of the system is a two-frequency torus. An increase in the number of independent frequencies leads to an increase in the torus dimension and complication of dynamics. The classic examples of the transition to chaos as a result of the destruction of the torus are the Landau-Hopf scenario [6,7] and the Ruelle and Takens scenario [8]. As applied to turbulence, Landau assumed that the transition to chaos occurs through an infinite sequence of the creation of new frequencies (modes), and in the limit a complex chaotic behavior is born [6,7]. Later Ruelle and Takens [8] showed that the transition to chaos can also occur in the case of a small number of independent modes: the torus breaks down even in the case of two incommensurate frequencies and transforms into a strange chaotic attractor. As a result, by now there are a large number of works devoted to the study of the transition from a two-dimensional torus to chaos [9–11]. Later situations when tori with three or more frequencies are preserved were shown. A logical step in this direction is the study of the evolution of quasiperiodic oscillations of higher dimension. However, the study of the evolution of tori of dimension three and more turned out to be a much more difficult task, especially in experiment [12]. Professor Vadim Anishchenko was one of the first who study the destruction of a three-frequency torus [13–16].

Non-autonomous oscillators and ensembles of interacting oscillators are usually used as the simplest models demonstrating multi-frequency quasiperiodic oscillations. In [17], using the example of a network of globally coupled van der Pol oscillators, the possibility of implementing a sequence of quasiperiodic Hopf bifurcations was shown. However, in such a model the chaos domains are very small in the parameter space, and arise during the destruction of two-frequency tori. In [18], a model of a multi-circuit generator was proposed, in which the possibility of multi-frequency quasiperiodic oscillations, as well as the formation of chaotic dynamics, was demonstrated. The aim of the current work is to study the formation of chaotic dynamics in a multi-circuit generator [18] in the case when tori with different numbers of incommensurate frequencies are destroyed.

The work is structured as follows. In Section 2 a mathematical model of a multi-circuit generator is presented, the structure of the parameter plane of a multi-circuit generator is analyzed, the domains of quasiperiodic oscillations with different numbers of incommensurable frequencies are localized, the types of chaotic dy-

* Corresponding author.
E-mail address: stankevichnv@mail.ru (N.V. Stankevich).

https://doi.org/10.1016/j.chaos.2021.110998
0960-0779/

namics are classified depending on the spectrum of Lyapunov exponents. Section 3 is devoted to the investigation of chaotic attractors arising according to various scenarios: with the destruction of a two-frequency torus, as well as with the destruction of a four- and three-frequency tori. The analysis of quasiperiodic bifurcations with variation of the parameters of the system is carried out, the properties of various types of chaotic attractors are investigated.

2. Multi-mode generator as an object of study of multi-frequency quasiperiodic oscillations

A multi-circuit generator can be used as the simplest self-sustained generator in which multi-frequency quasiperiodic oscillations can be implemented. In [18] a model of a multi-circuit generator was proposed, in which the possibility of multi-frequency quasiperiodic oscillations, as well as the formation of chaotic dynamics was demonstrated. Such a generator consists of N oscillatory circuits coupled via a common positive feedback circuit. Each oscillatory circuit has its own frequency, as well as a parameter responsible for its excitation, i.e. for the excitation of each mode in the generator.

Mathematical model of such a generator can be written with the following system of differential equations:

$$\ddot{x}_i - (\lambda k_i - x_i^2)\dot{x}_i + \Delta_i x_i + \sum_{i=1}^{n} k_i \dot{x}_i - k_i \dot{x}_i = 0 \qquad (1)$$

where $i = (1 \,..\, N)$, the number of circuits in the generator, x_i, $\dot{x}_i$ are the dynamic variables of each oscillatory circuit. Each oscillatory circuit is a van der Pol type oscillator, in which the parameter λ is responsible for the excitation of self-oscillations in the circuit. The parameters Δ_i determine the frequencies of each oscillatory circuit.

Following [18] we will also consider the case of a five-circuit generator, i.e. $N = 5$ with an irrational ratio of all natural frequencies distributed as: Δ_1=1, Δ_2=$\sqrt{3}$, Δ_3=$\sqrt{11}$, Δ_4=$\sqrt{41}$, Δ_5=$\sqrt{153}$.

The main tool for analyzing complex oscillatory modes, including chaotic and quasiperiodic, is the analysis of the full spectrum of Lyapunov exponents [19]. Analysis of the spectrum of Lyapunov exponents allows: to identify chaotic oscillations; diagnose quasiperiodic oscillations with different numbers of incommensurate frequencies; determine the type of quasiperiodic bifurcation (Hopf or saddle-node) [4,20,21]; to classify different types of chaotic dynamics.

A preliminary analysis of the five-circuit generator (1) showed [18] that in such a system, quasiperiodic oscillations with a different number of frequency components from five to one are possible. Moreover with an increase in the parameters responsible for the gains of each mode, the system retains only two-frequency quasiperiodic oscillations and chaos resulting from the destruction of a two-frequency torus with one positive and one zero Lyapunov exponents. At small values of the amplification coefficients quasiperiodic oscillations with a different number of incommensurate frequencies are preserved (for $N = 5$ with three, four, and five frequencies), and when they are destroyed, not only chaotic oscillations, but also hyperchaotic ones are formed.

Fig. 1 shows a chart of Lyapunov exponents and its enlarged fragments for a model of a five-circuit generator (1). These charts were constructed as follows: for each point of the parameter plane, the full spectrum of Lyapunov exponents was calculated in accordance with the Benetin algorithm [22], depending on the values of the exponents, a point on the parameter plane was colored in one or another colors, in accordance with the palette shown in the Fig. 1. The spectrum signature and symbolic designation are also presented in Table 1. As mentioned earlier, the circuit frequencies were separated from each other, with each of the amplification coefficient responsible for exciting each of the modes. Thus, the gain of each circuit introduces an additional oscillatory mode into the dynamics of the system. In our numerical experiments, we fixed the gains of the second, third, and fourth oscillatory circuits to be the same, rather small, and monitored the dynamics as the gains of the first and fifth circuits were varied. Fig. 1 shows charts for $k_2 = k_3 = k_4 = 0.5$.

In accordance with the spectrum of Lyapunov exponents, we identified two types of chaotic dynamics that were found in the system under consideration: (i) chaos with one positive, one zero, and eight negative Lyapunov exponents (black); (ii) hyperchaos with two positive, one zero and seven negative Lyapunov exponents (white). In numerical experiments, when constructing charts of Lyapunov exponents, we fixed the threshold of equality of Lyapunov exponents to zero equal to 0.001, i.e. if $|\Lambda_i| < 0.001$, then we assume that the exponent is zero. Moreover, in the case when we observe several zero exponts (for quasiperiodic oscillations), they will have a different order, but with an increase in the calculation accuracy, they will approach zero. For one-parameter plots of Lyapunov exponents, we increased the accuracy of calculating Lyapunov exponents.

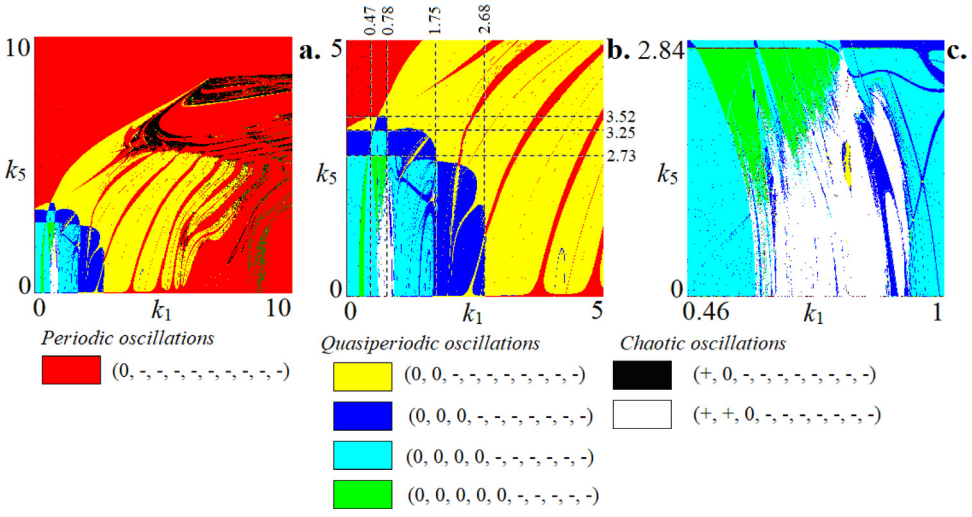

Fig. 1. Chart of Lyapunov exponents (**a.**) and it zoomed fragments (**b.** and **c.**)for multi-circuit generator (1)at Δ_1=1, Δ_2=$\sqrt{3}$, Δ_3=$\sqrt{11}$, Δ_4=$\sqrt{41}$, Δ_5=$\sqrt{153}$, λ=1, k_0=1, k_2= k_3= k_4= 0.5.

Table 1
Accordance of the dynamic regime, the signature of the spectrum of Lyapunov exponents and its symbolic notation.

Dynamic regime	Symbolic Notation	Signature of the spectrum of Lyapunov exponents
Periodic regime	P	(0, -, -, -, -, -, -, -, -)
Two-frequency quasi- periodic regime	T_2	(0, 0, -, -, -, -, -, -, -)
Three-frequency quasi- periodic regime	T_3	(0, 0, 0, -, -, -, -, -, -)
Four-frequency quasi- periodic regime	T_4	(0, 0, 0, 0, -, -, -, -, -)
Five-frequency quasi- periodic regime	T_5	(0, 0, 0, 0, 0, -, -, -, -)
chaos	C	(+, 0, -, -, -, -, -, -, -)
Hyperchaos	HC	(+, +, 0, -, -, -, -, -, -)

Let us turn to the description of the charts of Lyapunov exponents. Fig. 1a shows a chart in wide ranges of variation of parameters and two of its enlarged fragments visualizing the regions of multi-frequency quasiperiodic regimes (Fig. 1b) and regions of chaotic oscillations arising as a result of the destruction of multi-frequency tori (Fig. 1c).

As can be seen from Fig. 1a, model (1) demonstrates a variety of quasiperiodic and chaotic oscillations; periodic oscillations are also observed. At small values of the coefficients k_1 and k_5, quasiperiodic oscillations are observed with more than two frequency components. The parameter plane can be conventionally divided into rectangles with different numbers of frequency components (in Fig. 1b, we conventionally designated these rectangles with dotted lines). An increase in the coefficient of the operational amplifier of each of the circuits leads to a decrease in the number of frequencies, which corresponds to partial locking or suppression of the frequencies of various circuits. This phenomenon is typical for multi-mode oscillators and represents mode competition.

For small fixed k_1 ($k_1 < 0.47$), an increase in k_5 leads to a sequence of bifurcations, as a result of which quasiperiodic regimes change from four-frequency to two-frequency and then pass to periodic oscillations. At $0.78 > k_1 > 0.47$, as a result of varying k_5, it becomes possible to excite five-frequency quasiperiodic oscillations; however, the regions of five-frequency dynamics in the parameter space are rather small. The formation of chaotic dynamics as a result of the destruction of high-frequency tori is also observed. At $1.75 > k_1 > 0.78$, with a change in k_5, as well as at $k_1 < 0.23$, a transition from four-frequency tori to periodic oscillations is observed. At $k_1 \approx 1.75$, a transition to three-frequency oscillations is observed, which are transformed into two-frequency and then periodic with an increase of k_5 in interval $2.68 > k_1 > 1.75$. At $k_1 \approx 2.68$, a transition to two-frequency oscillations is observed, which will again transform into periodic ones with an increase in k_5. Similar bands of multi-frequency tori and transformations can be observed at fixed values of the operational amplifier k_5 and increasing the parameter k_1. The described transitions represent the competition between the modes of each oscillatory circuit. With an increase in the gain of one of the generators, its dominance and suppression of other modes are observed. Thus, in the complete system, periodic oscillations are observed in the mode of the suppressing circuit.

In the case when there is no dominance of only one oscillatory circuit, and the gains of the two oscillators are sufficiently large, we can speak of the interaction of two modes, which corresponds to two-frequency quasiperiodic oscillations on the parameter plane at $k_1 > 2.68$ and $k_5 > 3.52$. With further increase in the parameters k_1 and k_5, the development of chaotic dynamics is observed.

Thus two domains of chaos can be distinguished: (i) arising at large values of the coefficients k_1 and k_5; and (ii) for small values of the coefficients k_1 and k_5. Chaotic attractors of the first type appear as a result of the destruction of a two-frequency torus. In the second area, chaotic dynamics is based on the destruction of multi-frequency tori, while the dominant type of chaotic behavior in the second case is hyperchaos with two positive Lyapunov exponents. In the next section, we will consider in more detail the features of the formation and classification of chaotic attractors depending on the spectrum of Lyapunov exponents.

3. Features of chaotic dynamics

In a multi-circuit generator, two main types of chaotic oscillations can be distinguished, which are realized at large values of the parameters k_1 and k_5, which are generated as a result of the destruction of a two-dimensional torus, as well as those which are implemented at small k_1 and k_5 are generated as a result of the destruction of multidimensional tori. At large k_1 and k_5, chaos arises as a result of the destruction of the two-frequency torus in accordance with the Afraimovich-Shilnikov scenario. For small values of the parameters, tori with a large number of frequency components are destroyed; such attractors have their own peculiarities. For a more detailed analysis of scenarios for the destruction of multi-frequency tori and the features of the attractors themselves, we turn to a one-parameter analysis of the spectrum of Lyapunov exponents, Poincaré maps, and Fourier spectra.

3.1. Chaos formation as a result of a two-frequency torus destruction

Let us first consider a simpler and well-known situation of transition to chaos in accordance with the Afraimovich-Shilnikov scenario [23,24]. We fixed the gain values large enough. To localize regions of chaotic dynamics, we use one-parameter graphs of Lyapunov exponents, which are shown in Fig. 2a, b. Fig. 2a demonstrates graphs depending on the gain of the first oscillatory circuit. Fig. 2b shows a graphs for the case of a change in the gain of the fifth oscillatory circuit. Fig. 2c–g present the Poincaré maps by the hypersurface $\dot{x}_2 = 0$ in projection onto the dynamic variables of the first contour, demonstrating the development of chaotic dynamics with an increase in the parameter k_1. Similar Poincaré maps in Fig 2h–l show the development of chaotic dynamics with increasing parameter k_5.

With an increase in the parameter k_1 at $k_5 = 6.0$, on the basis of a cycle of period 1, a two-frequency torus is born (TR in Fig. 2a, c), which then collapses according to the Afraimovich-Shilnikov scenario and transforms into a chaotic regime. A characteristic feature of this scenario is the presence of synchronization tongues arising via saddle-node bifurcations at the threshold of chaos. Fig. 2d shows the Poincaré map for a cycle of period 7. This cycle undergoes a cascade of period-doubling bifurcations, which results in the formation of a 7-component chaotic attractor shown in Fig. 2f. As the parameter k_1 increases, the components of the attractor merge, forming a chaotic attractor corresponding to the destroyed base torus (Fig. 2f). With a further increase in the parameter k_1, the development of the chaotic attractor continues (Fig. 2g).

Fig. 2b illustrates the transition to chaos with an increase in the parameter k_5 for $k_1 = 7.0$. In this case, for small values of the coefficient k_5, there is a torus alternating with regions of periodic oscillations. However, the development of chaos on the basis of the torus is not observed. Fig. 2h and j show the Poincaré maps for

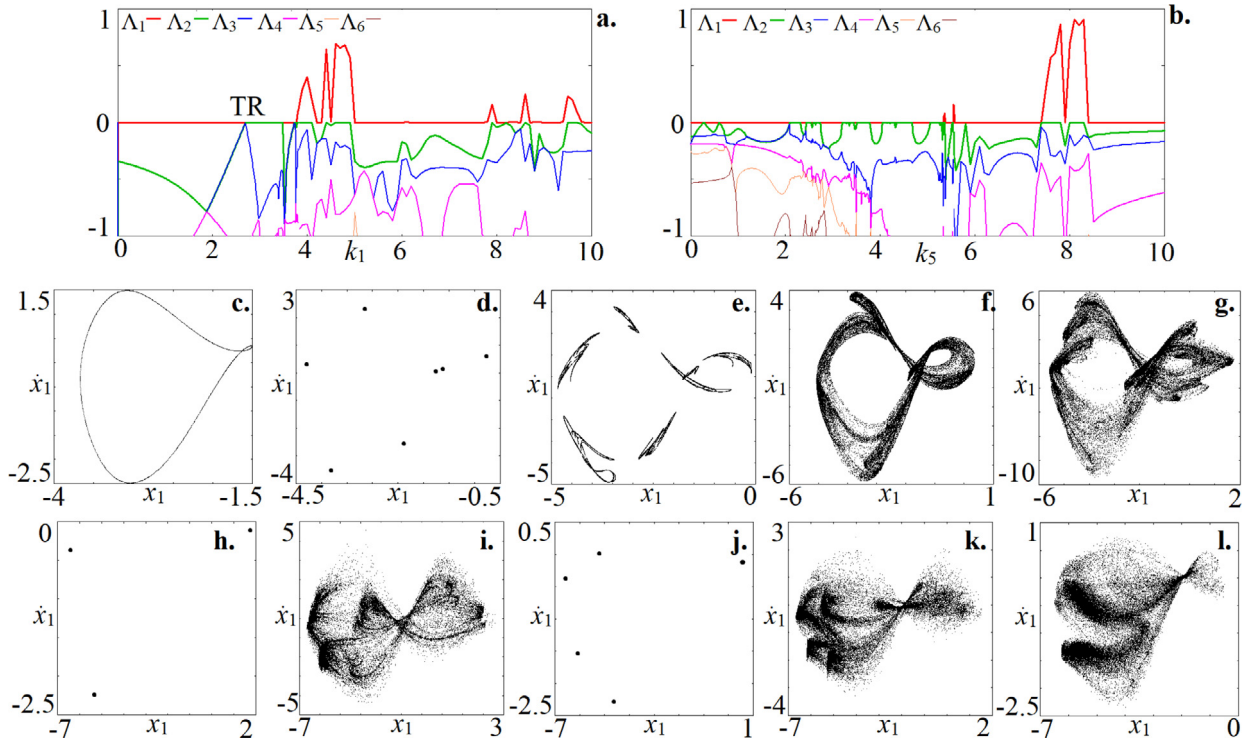

Fig. 2. Graphs of the six largest Lyapunov exponents for model (1): **a.** $k_5 = 6.0$, **b.** k_1=7.0. Poincaré maps for model (1): **c.** k_1=3.0, k_5=6.0; **d.** k_1=3.5, k_5=6.0; **e.** k_1=3.8, k_5=6.0; **f.** k_1=4.0, k_5=6.0; **g.** k_1=4.7, k_5=6.0; **h.** k_1=7.0, k_5=7.0; **i.** k_1=7.0, k_5=7.6; **j.** k_1=7.0, k_5=7.9; **k.** k_1=7.0, k_5=8.0; **l.** k_1=7.0, k_5=8.3. Other parameters: Δ_1=1, Δ_2=$\sqrt{3}$, Δ_3=$\sqrt{11}$, Δ_4=$\sqrt{41}$, Δ_5=$\sqrt{153}$, λ=1, k_0=1, k_2= k_3= k_4= 0.5.

period-3 and period-5 cycles. These cycles for sufficiently large values of the parameter k_5 ($k_5 > 7.5$) alternate with chaotic regimes (Fig. 2i, k). The structure of the Poincaré maps for the chaotic attractors under consideration preserves the shape of the destroyed base torus; however, it is inhomogeneous; condensations of points in the vicinity of limit cycles are clearly visible. With an increase in the parameter k_5, the chaotic attractor becomes more uniform (Fig. 2l); such an attractor corresponds to the maximum positive Lyapunov exponent. For all the examples presented, the chaotic attractor is characterized by one positive, one zero, and eight negative Lyapunov exponents.

3.2. Chaos formation as a result of a multi-frequency torus destruction

As mentioned above for small values of the gains of the circuits in the generator, multi-frequency tori with three, four, and five incommensurate frequencies are observed. The destruction of multi-frequency tori is a complex multidimensional task that involves many different problems, most of which are still open. It is clearly seen on the chart of Lyapunov exponents (Fig. 1) that in a multi-circuit generator (1) at low amplification coefficients, multi-frequency tori are destroyed, forming chaotic attractors. Fig. 1c shows an enlarged fragment of the chart in which we classified various types of chaotic behavior depending on the spectrum of Lyapunov exponents. The first feature that is characteristic of the chaos resulting from the destruction of multi-frequency tori is the presence of two positive Lyapunov exponents, the so-called hyperchaos. For a more detailed analysis, we again turn to one-parameter plots of Lyapunov exponents and Poincaré maps.

Fig. 3 shows a graphs of the six largest Lyapunov exponents depending on the gain k_1 at k_5=0.65, $k_2 = k_3 = k_4 = 0.5$. At small values of the coefficient k_1, a four-frequency quasiperiodic regime is observed; it corresponds to the equality of the four largest Lyapunov exponents to zero. In this case, the next two negative exponents (Λ_5, Λ_6) are the same in their absolute value. At $k_1 \approx 0.236$, the indicators Λ_5 and Λ_6 approach zero, after which the fifth indicator remains zero, and the sixth again becomes negative. Such a change in the Lyapunov exponents indicates that a five-dimensional torus has arisen in the system as a result of the quasiperiodic Hopf bifurcation (QH) [4,20,21]. The five-dimensional torus remains stable up to $k_1 \approx 0.34$, at which, as a result of the saddle-node quasiperiodic bifurcation (QSN1), it is transformed again into a four-frequency torus. In the interval k_1 (0.55-1), the formation of chaotic dynamics is observed, which we will consider in more detail below (Fig. 4).

An interesting dynamics of the Lyapunov exponents is observed in the interval of the parameter k_1 (1.68-1.76), see Fig. 3b. At $k_1 = 2$, a three-frequency quasiperiodic regime is implemented with three zero Lyapunov exponents, the fourth and fifth are negative and are equal to each other in absolute value. In the vicinity of $k_1 \approx 1.736$ (Fig. 3b), the fourth and fifth indicators become different, the fourth approaches zero, but then becomes negative (QD). Such dynamics of the Lyapunov exponents is characteristic of the torus doubling bifurcation. However, the fourth exponent does not become zero. Fig. 3c-d shows the Poincaré maps in a single Poincaré section with a hypersurface $\dot{x}_1 = 0$ (fragments **1.**) and two projections of the map in a double section with hypersurfaces: $\dot{x}_1 = 0$, $x_4 = 0$ (fragments **2.** and **3.**) for two values of the parameter k_1: before ($k_1 = 1.78$, Fig. 3c) and after ($k_1 = 1.71$, Fig. 3d) point QD. As can be seen from the projections onto the plane of the first contour, both attractors correspond to a three-frequency invariant torus, the invariant curve in a double section is clearly visible (Fig. 3c1). The invariant curve has a discontinuity, this feature is associated with the choice of the section plane. As the parameter k_1 decreases, we pass through the point QD, and Fig. 3d shows similar illustrations for the point $k_1 = 1.71$. The invariant curve in the double section has become more complicated, but at

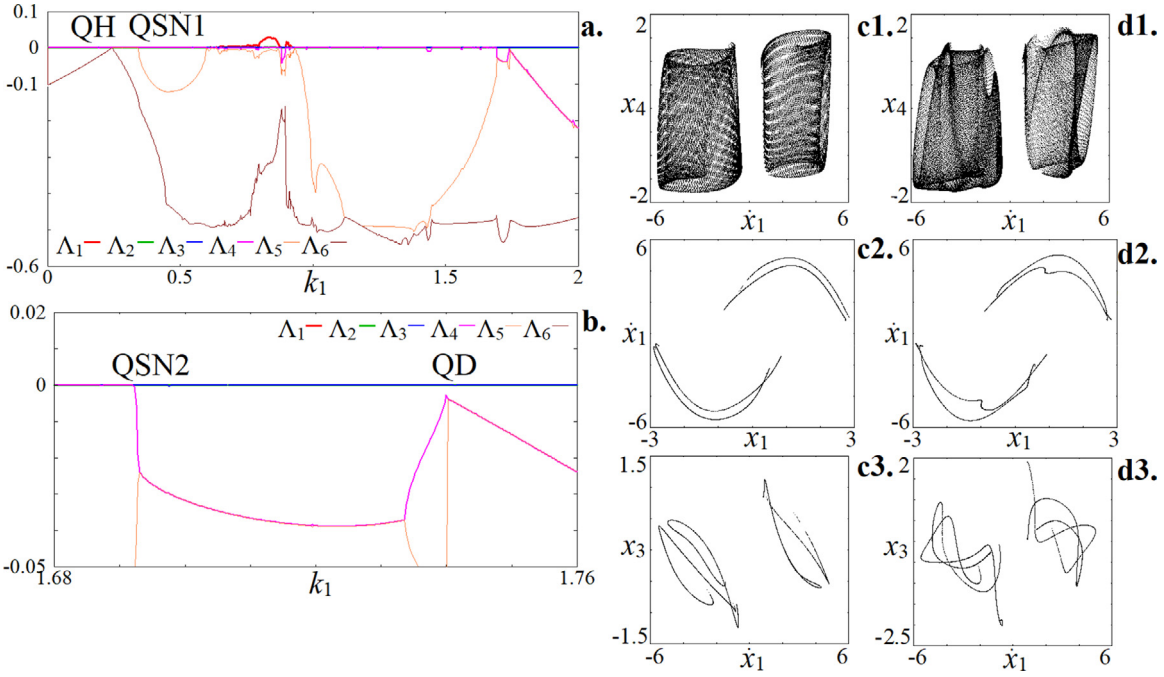

Fig. 3. Graphs of the six largest Lyapunov exponents for model (1): **a., b.** $k_5 = 0.65$. Poincaré maps for model (1): **c.** k_1=1.78; **d.** k_1=1.71. Other parameters: Δ_1=1, Δ_2=$\sqrt{3}$, Δ_3=$\sqrt{11}$, Δ_4=$\sqrt{41}$, Δ_5=$\sqrt{153}$, λ=1, k_0=1, k_2= k_3= k_4= 0.5, k_5= 0.65. **c1., d1**. - cross-section hypersurface $\dot{x}_1 = 0$; **c2., c3., d2., d3**. - double Poincaré section with hypersurface $\dot{x}_1 = 0$, $x_4 = 0$.

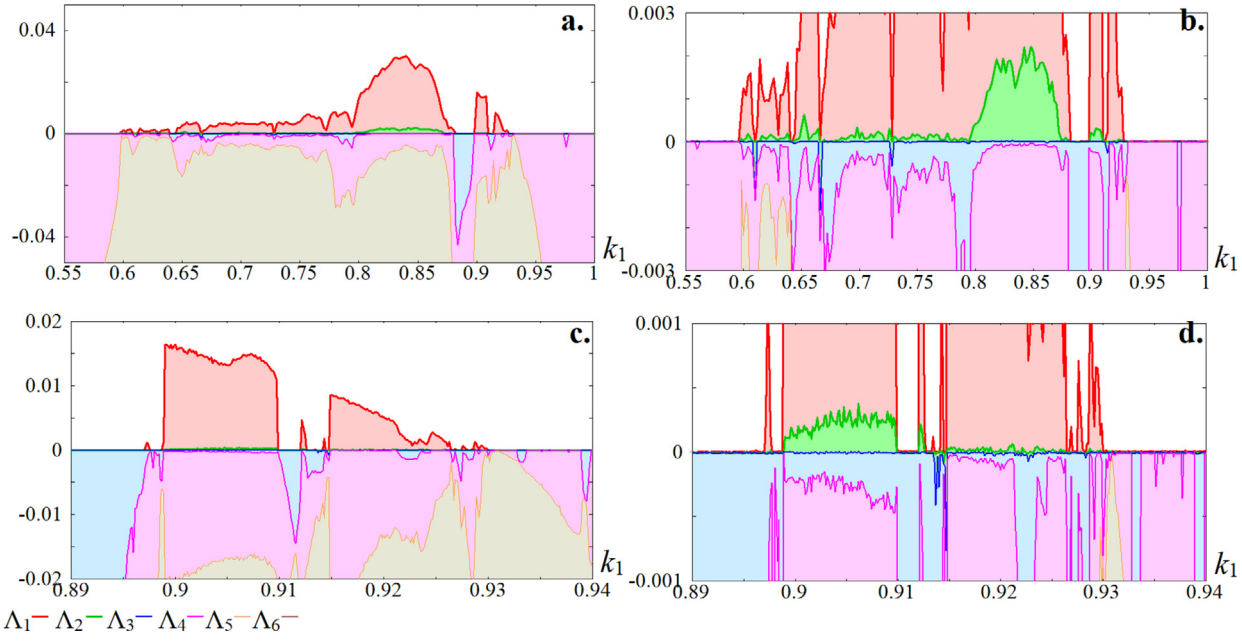

Fig. 4. Graphs of the six largest Lyapunov exponents for model (1) in the domain of hyperchaos. Parameters: Δ_1=1, Δ_2=$\sqrt{3}$, Δ_3=$\sqrt{11}$, Δ_4=$\sqrt{41}$, Δ_5=$\sqrt{153}$, λ=1, k_0=1, k_2= k_3= k_4= 0.5, k_5= 0.65.

the same time it retained its smooth continuous shape. However, in projection onto other variables, the invariant curve in the double section has changed, thus we can conclude that the winding number of the three-frequency torus has changed. With a further decrease in the gain k_1, we observe a transition to a four-frequency torus via a saddle-node bifurcation at $k_1 \approx 1.69$ (QSN2).

Let us consider in more detail the features of the formation of complex dynamics in the interval (0.55-1). We construct an enlarged fragment of the graphs of Lyapunov exponents, shown in Fig. 4a, b with different scales along the ordinate axis. On the enlarged fragment, two regions of chaos are detected, the first arises from a four-frequency torus, the second from a three-frequency one (Fig. 4c, d).

A feature of the chaos resulting from the destruction of multi-frequency tori is that the largest Lyapunov exponent is rather small. The maximum value of the largest Lyapunov exponent in the considered interval reaches 0.03. If we compare with the chaos studied in Section 3.1, then these numbers differ by a factor of 10. In Fig. 4a, it can also be noted that the second, third and fourth exponents (Λ_2, Λ_3, Λ_4) are close to zero. To refine these exponents, Fig. 4b shows an enlarged fragment in the vicinity of the zero value of the Lyapunov exponent. It is clearly seen that the

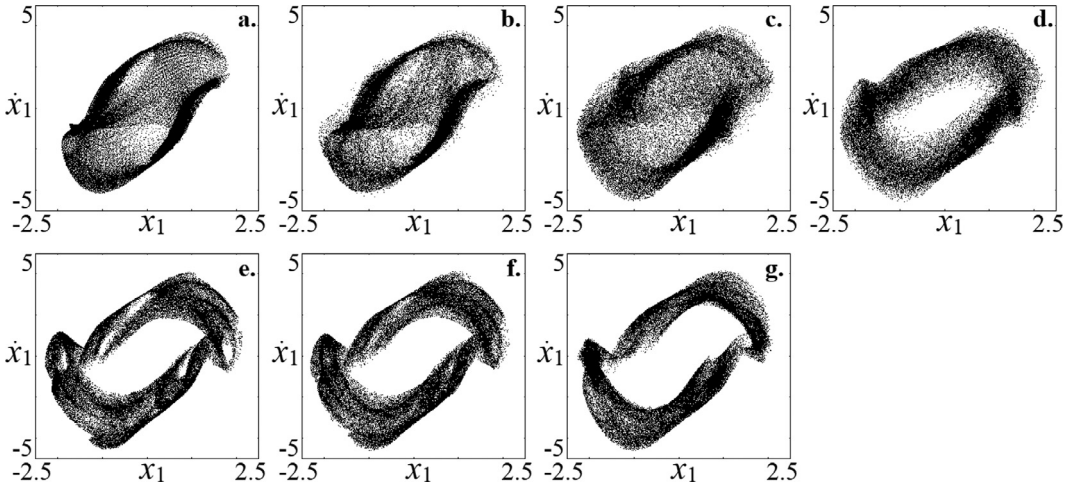

Fig. 5. Poincaré maps for model (1): **a.** k_1=0.58; **b.** k_1=0.6; **c.** k_1=0.7; **d.** k_1=0.85; **e.** k_1=0.89; **f.** k_1=0.9; **g.** k_1=0.92. Other parameters: Δ_1=1, Δ_2=$\sqrt{3}$, Δ_3=$\sqrt{11}$, Δ_4=$\sqrt{41}$, Δ_5=$\sqrt{153}$, λ=1, k_0=1, k_2= k_3= k_4= 0.5, k_5= 0.65. Cross-section hypersurface $\dot{x}_1 = 0$.

second Lyapuniv exponent (Λ_2) is weakly positive, the third (Λ_3) is zero, and the fourth (Λ_4) is weakly negative. The second positive Lyapunov exponent reaches the maximum value of 0.002, in a fairly large interval of the parameter, the value of the exponent is less than 0.001, while it is still well distinguishable from zero. The values of the weakly negative fourth exponent (Λ_4) are slightly higher in absolute value, while still at most points of the parameter interval they are less than 0.003. This feature can be explained by the fact that during the development of chaotic dynamics, various bifurcations of multi-frequency tori are observed, which are associated with the appearance of saddle tori with different numbers of frequency components, which will have multi-dimensional neutral manifolds. For example, this is possible with a saddle-node quasiperiodic bifurcation of a three-frequency torus. Neutral manifolds will contribute to chaotic behavior, which will give Lyapunov exponents close to zero.

Fig. 4c, d show a fragment of the plots of Lyapunov exponents for the second region of chaos, where a transition to chaos from the three-frequency quasiperiodicity regime is observed. As in the previous case, the largest Lyapunov exponent is of the order of 10^{-2}, and the second, third and fourth are difficult to distinguish from zero. An increase in scale (Fig. 4d) allows us to diagnose an weak hyperchaos in this case.

Fig. 5 shows typical attractors in the Poincaré section with the hypersurface $\dot{x}_1 = 0$ in the projection onto the variables of the first circuit for multi-frequency tori and hyperchaotic attractors developed on their basis. Fig. 5a shows an example of a four-frequency torus, 5b - 5d - chaos born on the basis of T_4 with an increase in the parameter k_1 and its development with an increase in the largest Lyapunov exponent. As a result of the transition to chaos, the Poincaré map becomes blurred. This feature indicates the presence of neutral manifolds in a chaotic attractor. With an increase in the coefficient k_1, an increase of the two largest Lyapunov exponents is observed; in this case, points of the map don't visit a region in the vicinity of zero.

An example of a three-frequency torus is shown in Fig. 5e. The phase portrait is blurred, while keeping the boundaries of the two-dimensional torus. Chaotic attractors resulting from the destruction of a three-dimensional torus are shown in Fig. 5f, g. As can be seen in this case, the points in the Poincaré map do not visit the vicinity of zero. The development of chaos vanishes its structure, but the attractor itself remains in the vicinity of the three-dimensional torus.

3.3. Comparative analysis of the spectral properties of chaotic attractors

Let us consider the features of chaotic attractors of each type. As a signal analysis tool, we will use the projections of attractors in the Poincaré section and the Fourier spectra. Fig. 6 shows these illustrations for four different chaotic attractors. For each case, fragment **1** demonstrates the projection of the Poincaré map onto the plane of dynamic variables of the first contour. Fragments **2, 3, 4, 5** show projections onto dynamic variables of various contours: first-second, first-third, first-fourth and first-fifth. Such cross projections are somewhat analogous to Lissajous figures and allow conclusions to be drawn about synchronization between oscillatory circuits. In the case of full in-phase synchronization, the Lissajous figure is a diagonal line. Fragment **6** shows the Fourier spectrum of the signal, which was calculated for the summary signal from all contours. Table 2 shows the values of the six largest Lyapunov exponents and the Kaplan-Yorke dimension for the attractors under consideration.

The first two examples (Fig. 6a and b) relate to the chaos that arose at large values of the gain, respectively, via the destruction of the two-frequency torus. The two remaining ones are for small values of the amplification coefficients and via the destruction of multifrequency tori, accordingly.

During the destruction of a two-frequency torus, we observed two types of chaotic attractors. Fig. 6a shows an example of an attractor that arose as a result of a cascade of bifurcations of period-doubling of a cycle of period-7. As a result of a cascade of period-doubling bifurcations, a 7-component chaotic attractor arises. This attractor has a thin linear structure, which indicates that there is only one unstable manifold. The Fourier spectrum contains a spectral component at the frequency of the base mode of self-oscillation. This frequency corresponds to the frequency of the first mode, which suppressed all others as a result of competition. Discrete components in the oscillator spectrum are the highest multiples of the frequency components. The power spectrum has a typical form for a chaotic attractor born in accordance with the Feigenbaum scenario [25]. Fig. 6b illustrates the developed chaos upon the destruction of a two-frequency torus. As a result of the homoclinic bifurcation, 7 components of the chaotic attractor merged and the attractor corresponds to the destroyed two-frequency torus. The attractor in the Poincaré section has the shape of blurred regions, which in turn indicates the presence of

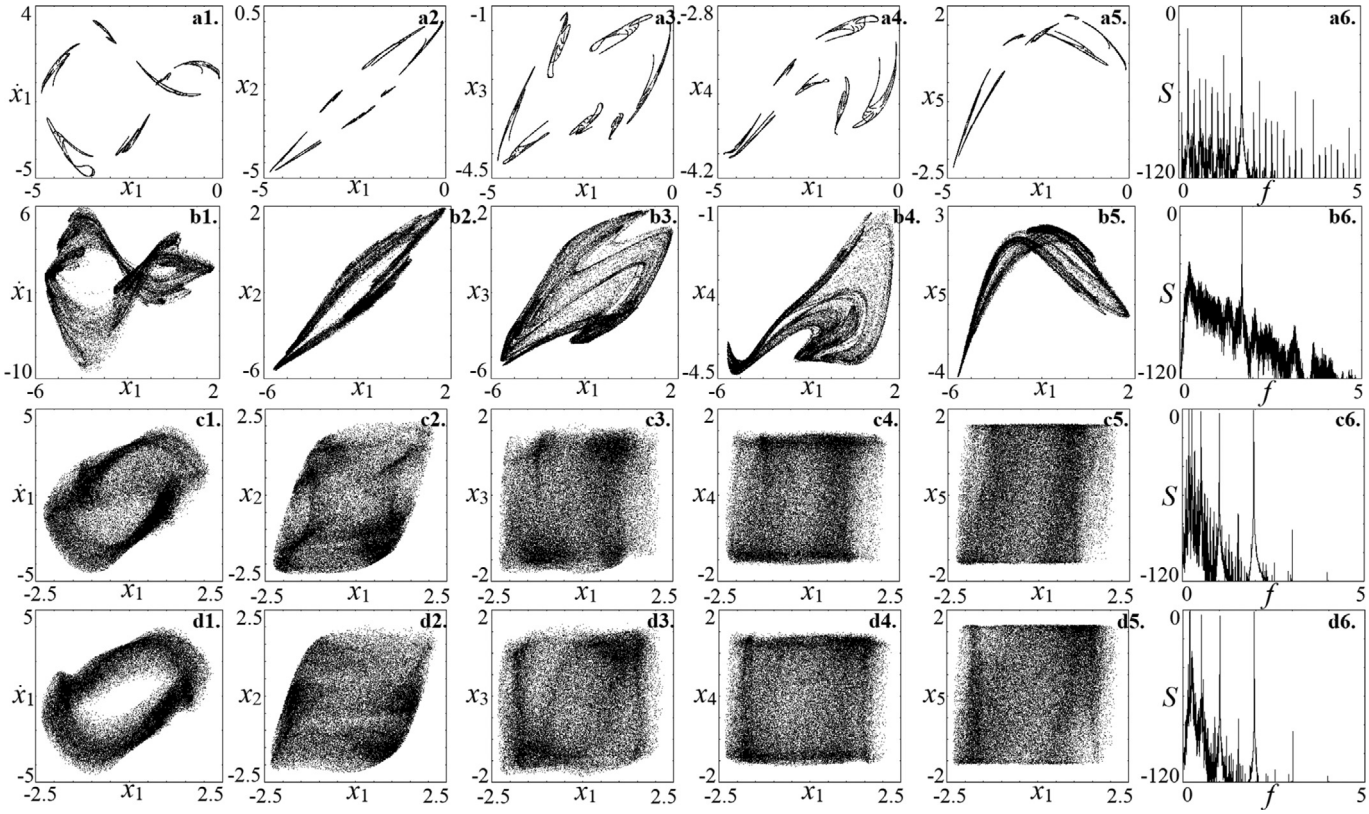

Fig. 6. Poincaré maps for model (1) and Fourier spectrums: **a.** k_1=3.8, k_5=6.0; **b.** k_1=4.7, k_5=6.0; **c.** k_1=0.7, k_5=0.65; **d.** k_1=0.85, k_5=0.65. Other parameters: Δ_1=1, Δ_2=$\sqrt{3}$, Δ_3=$\sqrt{11}$, Δ_4=$\sqrt{41}$, Δ_5=$\sqrt{153}$, λ=1, k_0=1, k_2= k_3= k_4= 0.5, k_5= 0.65. Cross-section hypersurface $\dot{x}_1 = 0$.

Table 2
Values of the six largest Lyapunov exponents and the Kaplan-Yorke dimension for various chaotic attractors.

k_1	k_5	Λ_1	Λ_2	Λ_3	Λ_4	Λ_5	Λ_6	D_KY
3.8	6.0	0.0809	0.0	-0.2552	-0.8771	-2.1468	-2.7364	2.32
4.7	6.0	0.5847	0.0	-0.2143	-0.7175	-2.3459	-3.5741	3.52
0.7	0.65	0.0041	0.0001	0.0	-0.0004	-0.0049	-0.4858	4.78
0.85	0.65	0.0262	0.0019	0.0	-0.0001	-0.0063	-0.3065	5.07

an unstable two-dimensional manifold. The fact that the attractor in Fig. 6b2 is compressed in the transverse direction indicates the effect of synchronization between the first and second modes of the oscillator. At the same time, the Fourier spectrum contains an expressed harmonic corresponding to the base mode that survived as a result of competition. However, the rest of the discrete components disappeared, the spectrum became more uniform and broadband. The spectrum of Lyapunov exponents contains one positive exponent. With the development of chaotic dynamics, the largest exponent grows and can reach values of the order of unity. It is also worth noting that the fifth and sixth indicators have negative values, rather large in absolute value, which indicates the presence of strongly dissipative directions. The transition from a thin linear structure seven-component attractor to one attractor leads to an increase in the Kaplan-Yorke dimension by one, which confirms the presence of two-dimensional unstable manifolds in the attractor shown in Fig. 6b.

Next, let us analyze the chaotic attractors resulting from the destruction of multi-frequency tori at small values of the amplification coefficients of the circuits. Fig. 6c shows a chaotic attractor that appears as a result of the destruction of a four-frequency torus, in Fig. 6d destroyed three-frequency torus is presented. The shape of the attractor in the Poincaré section in the projection onto the plane of the dynamic variables of the first circuit is clearly different from the case of the destruction of the two-frequency torus, the phase points are not concentrated in the vicinity of the invariant curve of the two-frequency torus. The projections of the phase portraits show less synchronization between the first and second oscillatory circuits and a lack of synchronization between the first and all the others. Fourier spectra for destroyed multi-frequency tori contain independent spectral components of multi-frequency tori. Five frequency components are diagnosed in the spectrum of a chaotic attractor born as a result of the destruction of a four-frequency torus (Fig. 6c). Four components are observed in the spectrum for chaos based on a three-frequency torus (Fig. 6d). High-frequency components for chaos based on multi-frequency tori are suppressed.

The values of positive Lyapunov exponents for chaos resulting from the destruction of multi-frequency tori are much smaller, which indicates weak chaos, but the calculation confirms two positive Lyapunov exponents. It is also clearly seen that the fifth and sixth indicators are also small, which indicates that strong dissipation has not yet appeared in these directions. Such a spectrum is characteristic of multi-dimensional chaos, as a result of which we see an increase in the Kaplan-Yorke dimension of the chaotic attractor, and it can exceed 5.

4. Conclusion

An example of a multi-mode self-oscillator containing five eigen-modes is used to study the features of the formation of chaotic dynamics upon destruction of quasiperiodic oscillations with different number of incommensurate frequencies. Two types of chaotic attractors are illustrated.

The first type arises at large values of the parameters responsible for the gains of the circuits in the generator and corresponds to the regime when one of the modes dominates as a result of competition between the oscillatory modes of the circuits. This type of chaos develops as a result of the destruction of the two-frequency torus according to the Afraimovich-Shilnikov scenario, including the sequence of period-doubling bifurcations of the limit cycle formed as a result of synchronization on the two-frequency torus, which in turn corresponds to the synchronization of all eigenmodes of the oscillator. A developed chaotic attractor has one positive Lyapunov exponent, the value of which is enough large (more then 10^{-1}). The Kaplan-York dimension of such a chaotic attractor can vary from 2 to 4.

The second type of chaos arises at small values of the parameters responsible for the gains of the circuits in the generator and corresponds to the regime when all eigenmodes are independent, which leads to the formation of four and five-dimensional tori. This type of chaos develops as a result of the destruction of multi-frequency tori. The Fourier spectrum of such a chaotic attractor contains discrete components corresponding to the modes of the contours. Chaotic dynamics in this case is characterized by two positive Lyapunov exponents (so-called hyperchaos), while the second positive exponent is significantly less than the first. Despite the fact that chaos is weak, it is multi-dimensional chaos, as evidenced by the Kaplan-York attractor dimension of more than 5.

Funding

The work was carried out with the financial support of the Russian Science Foundation, grant no. 21-12-00121 (Sect.1, 2, 3.1, 4). Work of NVS was partially supported by the grant of Russian Foundation for Basic Research, grant no. 19-31-60030 (Sect.3.2).

Declaration of Competing Interest

The authors declare that they have no known competing financial interests or personal relationships that could have appeared to influence the work reported in this paper.

References

[1] Anishchenko VS. Dynamical chaos: models and experiments: appearance routes and structure of chaos in simple dynamical systems (Vol. 8) 1995.
[2] Pikovsky A, Kurths J, Rosenblum M, Kurths J. Synchronization: a universal concept in nonlinear sciences. Cambridge university press; 2003. No. 12.
[3] Landa PS. Nonlinear oscillations and waves in dynamical systems (Vol. 360). Springer Science & Business Media; 2013.
[4] Broer HW, Huitema GB, Takens F, Braaksma BLJ. Unfoldings and bifurcations of quasi-periodic tori. American Mathematical Soc; 1990. No. 421.
[5] Anishchenko VS, Vadivasova T, Strelkova G. Deterministic nonlinear systems. A short course, 294. Switzerland: Springer International Publishing; 2014.
[6] Landau LD. On the problem of turbulence. Dokl Akad Nauk SSSR 1944;44:339 [in Russian].
[7] Hopf E. A mathematical example displaying features of turbulence. Commun Pure Appl Math 1948;1(4):303–22.
[8] Ruelle D, Takens F. On the nature of turbulence. Commun Math Phys 1971;20:167–92. doi:10.1007/BF01646553.
[9] Grebogi C, Ott E, Yorke JA. Are three-frequency quasiperiodic orbits to be expected in typical nonlinear dynamical systems? Phys Rev Lett 1983;51(5):339.
[10] Grebogi C, Ott E, Yorke JA. Attractors on an N-torus: quasiperiodicity versus chaos. Physica D: Nonlinear Phenomena 1985;15(3):354–73.
[11] Grebogi C, Ott E, Pelikan S, Yorke JA. Strange attractors that are not chaotic. Physica D: Nonlinear Phenomena 1984;13(1-2):261–8.
[12] Stankevich NV, Kuznetsov AP, Popova ES, Seleznev EP. Experimental diagnostics of multi-frequency quasiperiodic oscillations. Commun Nonlinear Sci Numer Simul 2017;43:200–10.
[13] Anishchenko VS, Letchford TE, Safonova MA. Critical phenomena in the harmonic modulation of two-frequency self-excited oscillations-Transitions to chaos through a three-torus. Pisma v Zhurnal Tekhnischeskoi Fiziki 1985;11:536–41.
[14] Anishchenko VS, Letchford TE. Destruction of Trifrequent oscillations and the chaos in the generator during the biharmonic effect. Zhurnal Tekhnicheskoi Fiziki 1986;56(11):2250–3.
[15] Anishchenko VS, Safonova MA, Feudel U, Kurths J. Bifurcations and transition to chaos through three-dimensional tori. Int J Bifurc Chaos 1994;4(03):595–607.
[16] Feudel U, Safonova MA, Kurths J, Anishchenko VS. On the destruction of three-dimensional tori. Int J Bifurc Chaos 1996;6(07):1319–32.
[17] Kuznetsov AP, Kuznetsov SP, Sataev IR, Turukina LV. About Landau–Hopf scenario in a system of coupled self-oscillators. Phys Lett A 2013;377(45–48):3291–5.
[18] Stankevich NV, Astakhov OV, Kuznetsov AP, Seleznev EP. Exciting chaotic and quasi-periodic oscillations in a multicircuit oscillator with a common control scheme. Tech Phys Lett 2018;44(5):428–31.
[19] Pikovsky A, Politi A. Lyapunov exponents: a tool to explore complex dynamics. Cambridge University Press; 2016.
[20] Vitolo R, Broer H, Simó C. Quasi-periodic bifurcations of invariant circles in low-dimensional dissipative dynamical systems. Regul Chaotic Dyn 2011;16(1):154–84.
[21] Stankevich NV, Kuznetsov AP, Seleznev EP. Quasi-periodic bifurcations of four-frequency tori in the ring of five coupled van der Pol oscillators with different types of dissipative coupling. Tech Phys 2017;62(6):971–4.
[22] Benettin G, Galgani L, Giorgilli A, Strelcyn JM. Lyapunov characteristic exponents for smooth dynamical systems and for Hamiltonian systems; a method for computing all of them. Part 1: theory. Meccanica 1980;15(1):9–20.
[23] Afraimovich VS, Shilnikov LP. Nonlinear dynamics and turbulence. Interaction Mech Math Ser 1983:1–34 1983.
[24] Gonchenko A, Gonchenko S, Kazakov A, Turaev D. Simple scenarios of onset of chaos in three-dimensional maps. Int J Bifurc Chaos 2014;24(08):1440005.
[25] Feigenbaum MJ. The onset spectrum of turbulence. Phys Lett A 1979;74(06):375–8.